Structure-property relations of triblock copolymer thermoplastics with interaction-tuned polymer additives

Karthika Madathil, Bishal Upadhyay, William K. Ledford, S.Michael Kilbey II, and Gila E. Stein, Y

yDepartment of Chemical and Biomolecular Engineering, The University of Tennessee at Knoxville, Knoxville, Tennessee 37996, United States

zDepartment of Chemistry, The University of Tennessee at Knoxville, Knoxville, Tennessee

37996, United States

E-mail: gstein4@utk.edu

Abstract

Block copolymer (BCP) thermoplastics are used in a wide range of commercial products. It is well known that the mechanical performance of these materials depends on the BCP architecture and composition, and the introduction of non-covalent interactions via comonomers can be used to tune key properties. However, tailoring the mechanics of BCPs by blending with polymeric additives is rarely explored, as most BCP/polymer blends have limited miscibility. Here, we examine the structure, mechanics, and thermal stability of a commodity thermoplastic, poly(styrene-b-ethylene-co-butylene-b-styrene) (SEBS), with polymeric additives of either polystyrene (PS) or poly(methyl methacrylate-co-cyclohexyl methacrylate) (PrC, 70 mol% cyclohexyl methacrylate). PS and PrC are athermal and enthalpically-compatible additives, respectively, for the polystyrene end-blocks in SEBS. The SEBS/PS blends have a narrow

miscibility window with respect to PS molecular weight and loading, where either an ordered lamellar morphology or a disordered morphology is observed. In contrast, the attractive interaction between PrC and polystyrene end-blocks leads to complete miscibility of SEBS/PrC blends across the full range of PrC molecular weights (up to 63.8 kg/mol) and loadings (up to 40 vol%) that were studied, where an ordered lamellar morphology with continuity in the rubber phase was generally observed. Consequently, the PrC additives can increase the modulus and yield stress, as well as delay the onset of strain hardening, without loss of toughness. Additionally, PrC additives can elevate the glass transition temperature of the PS blocks and maintain a high modulus at elevated operating temperatures, expanding the service window for SEBS. The principles established in this research could be translated to other types of styrenic BCP thermoplastics.

Keywords

SEBS, thermoplastic, elastomer, blend, self-assembly, mechanical properties, block copolymer

Introduction

Commodity block copolymer thermoplastics consist of glassy and rubbery blocks with high and low glass transition temperatures (T_g), respectively. The glassy domains act as physical cross-links in the rubbery matrix, producing a ductile material that can also be reprocessed above the T_g of the glassy block. The mechanical properties of BCP thermoplastics depend on the volume fractions of the glassy and rubbery domains and the BCP architecture. 1,2 ABA type triblock copolymers, consisting of glassy A domains as the minority phase and rubbery B domains as the matrix, have been extensively studied and commercially used for wide range of applications including adhesives, coatings, footwear, automobile parts and

medical devices.³⁵ A common ABA triblock copolymer platform has polystyrene end-blocks and polyisoprene, polybutadiene or poly(ethylene-co-butylene) as the midblock.⁶¹⁵ Thermoplastics based on poly(ethylene-co-butylene) or poly(ethylene-co-propylene) midblocks are particularly attractive, as the saturated rubber provides these materials with high oxidative and chemical stability.¹³

Numerous eorts have been directed towards understanding how the mechanical properties of BCP thermoplastics can be improved by modifying their architecture. For linear BCPs, domain bridging and looped entanglements in triblock and pentablock (ABA and ABABA) architectures will enhance the mechanical properties relative to AB diblock copolymers, wherein the domains are held together only by chain entanglements and van der Waals interactions. ^{2,16,17} In (AB)_n type alternating BCPs consisting of n AB block pairs, the tensile strength and modulus both increase with increasing n due to the presence of constrained, interconnected domains. 18,19 Branched architectures, such as miktoarm star polymers, can be exploited to form self-assembled structures with continuous rubbery domains at high volume fractions of the glassy polymer, 2022 resulting in materials with high elasticity along with high modulus. Another molecular design strategy is to introduce physical cross-links in one of the BCP domains by incorporating low amounts of hydrogen-bonding ²³²⁶ or ionic ^{27,28} comonomers. These cross-links can be incorporated in the soft block 2325,27,28 or the glassy block²⁶ to enhance the mechanical properties. Relatively fewer works have explored tailoring mechanical properties of BCPs by blending with polymeric additives, despite it being a simple strategy that could be compatible with commercially available BCPs and common processing methods. The main challenge with this strategy is nding a polymer additive that is miscible with one of the domains.

The phase behaviour of BCP/homopolymer blends has been well-studied over the past several decades. In a blend of an AB diblock copolymer with A homopolymer, the phase behaviour is mainly governed by entropic interactions arising from the relative chain lengths of the A homopolymer (N_h) and the A block in the BCP ($N_{A,BCP}$), given by

= $N_h = N_{A,BCP}$. ²⁹³³ For values of < 1, the A homopolymer is distributed throughout the A block of the BCP, driving both axial stretching and lateral expansion of the domain. The axial stretching of the BCP chain produces a conformational entropy loss that increases with the volume fraction of the homopolymer () in the blend. At a certain , this entropic penalty produces a change in interfacial curvature that drives an order-order phase transition (OOT). ³⁴³⁶ For 1, there is a loss in the combinatorial entropy of mixing from the increase in homopolymer chain length, and so the homopolymer chains will accumulate at the center of the A-domain bilayer. ³⁷ For 1, the entropic penalty drives macrophase separation of the homopolymer from the BCP system. ³⁸ For a given , the which marks the onset of macrophase separation will depend on the structure of the pure BCP, which is a function of f and N, where f_A is the volume fraction of the A block, is the Flory-Huggins parameter, and N is the degree of polymerization.

In a blend of an AB diblock copolymer or ABA triblock copolymer with type C homopolymer, where the C homopolymer is enthalpically compatible with the A block, the and at which the OOT and macrophase separation occur are each governed by two additional enthalpic interactions captured by $_{AC}$ (< 0) and $_{BC}$ (> 0). 3948 Experimental and theoretical studies have each shown that the phase behavior depends on the molecular weight of the A block and is largely unaected by the molecular weight of the C homopolymer. This is because in these blend systems, macrophase separation is mainly governed by the conformational entropic penalty of the A block and the homopolymer C, which is signicantly reduced with an increase in the molecular weight of the A block. 49,50 When the homopolymer additive is evenly distributed in the compatible block, which is anticipated for < 1, the A block undergoes axial stretching and lateral contraction at low , with an increase in the interfacial area per chain with increasing 39,44

Styrenic BCPs with poly(2,6-dimethyl-1,4-phenylene oxide) (PPO) homopolymer additive are a well-studied example of an ABA/C blend with $_{\rm AC}$ < 0. PPO homopolymer is fully miscible with PS homopolymer, 5156 and blends of styrenic BCPs and PPO are miscible for

> 1 provided the molecular weight of the PS block in the BCP is above 14 kg/mol. ^{49,50,57,58} The PPO additives tune the thermal stability and mechanical properties of the BCP, ^{58,59} increasing the modulus, ⁵⁸ tensile strength ⁵⁹ and strain-at-break point. ⁵⁹ However, PPO has some disadvantages as an additive, both in terms of practical applications and fundamental studies. BCP/PPO blends must be processed at temperatures above 250°C due to the high T_g of PPO. ⁵⁹ PPO is prepared by oxidative coupling, ⁶⁰ which produces high dispersity in molecular weight. ⁴³ Therefore, it is dicult to investigate the eects of additive molecular weight on its distribution within the A domains of the BCP and mesoscale ordering of the self-assembled domains.

Another potential polymer additive for styrenic BCPs is the copolymer poly(methyl methacrylate-co-cyclohexyl methacrylate) (PrC), which is miscible with PS homopolymer provided the composition of cyclohexyl methacrylate (CHMA) exceeds approximately 21 mol%. 56,6163 These PrC additives have Tg near that of PS (100 °C), and PS/PrC blends have a lower critical solution temperature of 220 °C, leading to a broad window for processing at moderate temperatures. Furthermore, PrC can be synthesized by controlled radical polymerization methods to achieve low dispersities (- 1.2). The enthalpic interaction between PrC and PS can be tuned by varying the copolymer composition, with the minimum in PrC,PS observed for approximately 70 mol% CHMA, 61 as shown in Figure S1. To the best of our knowledge, the miscibility of CHMA-based polymers with styrenic BCPs has not been explored.

This work describes a systematic investigation of PrC miscibility in poly(styrene-b-ethylene-co-butylene-b-styrene) (SEBS), a widely studied class of BCP thermoplastic. The PrC composition was xed at approximately 70 mol% CHMA, i.e., the composition that produces the strongest enthalpic compatibility with PS. The SEBS composition and molecular weight were also xed at 26 vol% styrene and $M_n = 103.5$ kg/mol, respectively. We selected a SEBS material with high styrenic content so the addition of miscible polymeric additives would produce a lamellar morphology. The lamellar morphology has a broad window of sta-

bility as a function of composition,⁶⁴ so the additive loading can be varied without inducing a change in interfacial curvature. Entropic eects that contribute to blend miscibility were explored by varying both the molecular weight of PrC, which changes, and its loading level dened by . PS homopolymer additives, i.e., athermal additives for the PS block in SEBS, were used as a control. The knowledge acquired from this study provides a framework to design miscible polymeric additives for styrenic BCP thermoplastics that manipulate nanoscale structure, bulk mechanics, and thermal stability without compromising processability.

Experimental

Materials SEBS was obtained from Sigma Aldrich. The number-average molecular weight $M_n = 103:5$ kg/mol and dispersity -= 1.05 were determined by gel permeation chromatography (GPC) relative to PS standards. The SEBS composition of 30 mol% PS was determined from 1H NMR. The SEBS composition on a volume basis is 26% polystyrene, assuming densities of 0.92 g/cm 3 and 1.05 g/cm 3 for poly(ethylene-co-butylene) and PS, respectively. The GPC trace and NMR spectrum for SEBS are shown in Figures S2 and S3, respectively.

PS samples with a range of molecular weights were purchased from Scientic Polymers and their molecular weights were veried by GPC. PrC samples were synthesized via reversible addition fragmentation chain transfer (RAFT) polymerization, adapting procedures described previously. For all RAFT polymerizations, the target copolymer composition, forman, was xed at 70 mol% CHMA, as it is reported as the minimum parameter for blends with PS. PrC molecular weight was varied by changing the total monomer concentration, and at the higher molecular weight, the feed ratio of CHMA:methyl methacrylate (MMA) had to be adjusted in order to hit the target composition. As an example, CHMA (64.4 mmol, 10.82 g), MMA (27.6 mmol, 2.76 g), 4-cyano-4-(phenylcarbonothioylthio)pentanoic acid (1 mmol, 279 mg), and AIBN (0.1 mmol, 16.8 mg) were dissolved in 10 mL of THF and added to 25mL round bottom ask equipped with a stir bar. The ask was sealed with a

septum and dissolved oxygen removed through three freeze-pump-thaw cycles. The ask was then immersed in a preheated oil bath set to 70 °C. After 18 h, the reaction was quenched by opening the ask to air and freezing the crude product mixture with liquid nitrogen. After thawing, the copolymer was isolated and puried by precipitation into cold methanol and gravity Itration. The recovered PrC copolymer was dried under vacuum for 24 h prior to use. Characterization by GPC and 1 H NMR showed that this PrC had a $M_n = 2,800$ g/mol, -=1.09, and 72 mol% CHMA. Characteristics of all PrCs synthesized are given in Table S1, along with GPC traces in Figure S4 and 1 H NMR spectra in Figure S5.

Polymer characterization ¹H NMR spectroscopy was used to conrm the composition of the SEBS BCP and the PrC random copolymers. In short, 10 mg of polymer was dissolved in d-chloroform and analyzed using a Varian 500 MHz spectrometer at room temperature. Gel permeation chromatography (GPC) was used to measure the molecular weight of the SEBS BCP, PrC copolymers, and PS homopolymers. The M_n and — of each polymer was determined at room temperature using an Agilent 1260 Innity II GPC system that used THF as the mobile phase at a ow rate of 1.0 mL/min. The GPC was equipped with triple detection consisting of an Optilab T-rEX dierential refractometer, a Viscostar III viscometry detector, and a Wyatt Dawn Helios multiangle light scattering detector. All molecular weights reported were obtained via conventional calibration analysis using polystyrene standards. Samples for GPC were prepared by dissolving 12 mg of polymer in 2 mL THF and then Itering the solution using 0.2 μM Iters.

Blend preparation Blends were prepared by mixing SEBS and polymer additive at different . Densities of 0.91 g/cm³ for SEBS, 1.00 g/cm³ for PS and 1.11 g/cm³ for PrC were used for calculating , assuming there is no volume change upon mixing. The polymer mixture was then dissolved in xylenes (98.5% purity) to produce a solution with 10 wt% polymer. Polymer Ims were prepared by bar coating the polymer solution onto a Mylar sheet using an Elcometer Im applicator with 500 m gap height. After drying in air at room

temperature, the Ims were cut to obtain rectangular pieces with 1 cm width and annealed in a vacuum oven for 48 hrs at 140 °C. The nal Im thicknesses after drying and annealing were 70-90 m. Films of neat SEBS (no additive) were also prepared by the same procedure.

Small-Angle X-ray Scattering (SAXS) A Xenocs GeniX 3D microfocus source with a copper target was used to produce a monochromatic beam with a 0.154 nm wavelength. The sample to detector distance was 0.9 m. A Pilatus3 R 300K detector (Dectris) with nominal pixel dimensions of 172 m 172 m was used for data acquisition. The data acquisition time was 5 min for all measurements. The two-dimensional images from each measurement were azimuthally integrated with SAXSGUI software to yield a one-dimensional scattering prole of intensity I (a.u) versus scattering vector q (nm⁻¹). In all the gures showing SAXS data, the plots from each data set have been vertically oset for clarity.

Transmission Electron Microscopy (TEM) TEM measurements were performed on Ims that were sectioned to a thickness of around 30 nm by a Leica EM FC7 microtome at -150 °C. The sections were placed on Nickel grids and stained with ruthenium tetroxide vapor for 15 min, which selectively stains the PS domain. The sample slices were imaged by a JEOL JEM 1400-Flash transmission electron microscope with an acceleration voltage of 120 kV.

Mechanical and thermal characterizations Room temperature tensile testing was performed using an Instron 5965 instrument. Experimental setup and data acquisition were performed using Bluehill version 4.18 software. The initial separation between the grips was 20 mm. The samples were uniaxially stretched at a strain rate of 1/min, with a crosshead speed of 20 mm/min, until break point. Tensile properties (modulus, yield stress, onset of strain hardening and toughness) were obtained from the stress-strain curves. Toughness was calculated from the area under the stress-strain curves. At least ve samples were measured for each blend composition, and the error bars in plots of tensile properties denote 1

standard deviation.

The stress-strain curves at elevated temperature, and the T_g 's of SEBS and SEBS/additive blends were all obtained using a TA instruments Q800 dynamic mechanical analyser (DMA) in tension mode under nitrogen atmosphere. The initial separation between the grips was 1 cm. To obtain stress-strain curves, the samples were equilibrated at 80°C and stretched at a strain rate of 1/min, corresponding to a crosshead speed of 10 mm/min. To obtain T_g , the experiments were run at a heating rate of 5 °C/min from 30 °C to 140 °C and an oscillating axial force with 1% strain amplitude at a frequency of 1 Hz was applied. The T_g was taken from the maximum of the tan curve.

The T_g 's of the PS and PrC additives were obtained using a TA instruments Q2000 dierential scanning calorimeter (DSC). A temperature range of 25 °C to 150 °C was used for heat-cool-heat cycles at a heating and cooling rate of 10 °C/min. The T_g was taken from the mid-point of the slope in the second heating cycle.

Results and Discussion

SEBS morphology

Prior to preparing blends of SEBS and polymer additives, the neat SEBS morphology was characterized using both SAXS and TEM. The SAXS data showed higher-order peaks at 2q[?], 3q[?] and 4q[?] positions, which are representative of an ordered lamellar (LAM) morphology, where q[?] is the position of the rst-order peak. TEM images for the SEBS sample, however, showed a perforated lamellar (PL) morphology having poorly ordered perforations (Figure S6). This is not surprising as the volume fraction of the PS block in SEBS is only 26%, which likely falls within the PL or cylindrical morphology regions in the phase diagram.⁶⁴ Furthermore, it has been noted in prior studies that the SAXS prole for PL morphology is not distinguishable from that of a LAM morphology when the perforations are poorly ordered.^{66,67}

Reproducibility

To check whether the structure obtained after annealing is an equilibrium morphology, SEBS/PS blend Ims were prepared by casting from dierent solvents: xylene, which has neutral selectivity to polystyrene and poly(ethylene-co-butylene) blocks, and cyclohexane, which is selective towards the poly(ethylene-co-butylene) block. 68,69 The SAXS proles obtained before and after annealing these Ims are shown in Figure S7. The as-cast structures are strongly dependent on the type of solvent used for casting the lm, where xylenes produces a more ordered structure than cyclohexane, as evidenced by the presence of a second-order peak. Xylenes also produces a larger domain periodicity than cyclohexane. After thermal annealing, the scattering patterns for both lms are similar: the primary peak position is the same, and the positions of higher-order peaks are consistent with lamellar symmetry. This outcome suggests that annealing drives both lms toward the same state. However, the lm cast from xylenes has sharper and stronger higher-order peaks, indicative of better domain ordering. Furthermore, when the blend is cast from xylenes, the domain periodicity before and after annealing is largely unchanged. This demonstrates that casting from a neutral solvent produces a state that is closer to equilibrium, and for this reason, xylenes was used for all Im processing. We also note that there is a variation of up to 3.5% in the lamellar periodicity for some of the samples when the same blend preparation method is repeated, as determined from SAXS measurements (shown in Figures S8-S9) and summarized in Figure S10.

Phase behaviour and morphology of SEBS/additive blends

Blends of SEBS with PS and PrC additives were prepared as a function of molecular weight and of the additives. Each SEBS/additive blend was dened by three parameters: (1) the type of additive used, PS or PrC; (2) the ratio of the length of additive to the length of a single polystyrene end-block in SEBS, ; and (3) the volume fraction of the additive in the

blend, . The following equation was used to calculate :

$$= \frac{N_{additive} \quad V_{additive}}{N_{PS,SEBS} \quad V_{styrene}}$$
 (1)

Wherein $N_{additive}$ and $N_{PS,SEBS}$ are the degrees of polymerization of the additives and a PS end-block in SEBS, respectively. For the SEBS used in this work, $N_{PS,SEBS}$ is 142. The $v_{additive}$ and $v_{styrene}$ terms are the monomer volumes for the additive and styrene, respectively, at the annealing temperature of 140 °C. The monomer volume was calculated using the M_n and density of the polymer at 140 °C. The density of the polymer at 140 °C was estimated using the density at 25 °C and a thermal expansion coecient of 710^{-5} /°C for both PS and PrC. In the case of PrC additive, $v_{additive}$ is the average monomer volume, accounting for the number of CHMA and MMA monomers in the chain. The volume of PS and PrC monomers at 140 °C were calculated to be 0.17 nm³ and 0.23 nm³, respectively. Table 1 provides a summary of all polymer additives used in this work, and also reports the value of without volume correction for reference, which is denoted as $^0 = N_{additive}/N_{PS,SEBS}$.

Table 1: Characteristics and relative sizes of additives

Additive type	f _{CHMA}	M _n (kg/mol)	_	0	1.6
PS	-		1.08	0.11	0.11
PS	-	3.8	1.07	0.26	0.26
PS	-	8.0	1.05	0.54	0.54
PS	-	12.0	1.05	0.81	0.81
PS	-	15.3	1.04	1.03	1.03
PS	-	19.5	1.05	1.32	1.32
PrC	0.72	2.8	1.09	0.13	0.18
PrC	0.73	4.4	1.08	0.21	0.28
PrC	0.76	10.0	1.16	0.47	0.63
PrC	0.74	12.5	1.12	0.60	0.80
PrC	0.78	17.0	1.16	0.80	1.07
PrC	0.74	18.5	1.13	0.87	1.17
PrC	0.75	21.0	1.16	0.98	1.32
PrC	0.76	27.5	1.16	1.29	1.73
PrC	0.66	34.8	1.16	1.70	2.28
PrC	0.76	63.8	1.16	3.00	4.02

Figures 1a report the phase behaviour of SEBS/additive blends over a wide range of and , where the markers on the phase diagram represent the blend compositions that were studied. F_H corresponds to the volume fraction of the hard phase in the blend, which includes both the additive and the polystyrene blocks of SEBS. F_H was calculated using 0.26 for the volume fraction of polystyrene in SEBS and assuming volume is additive after mixing. For the range of values examined (0.1-0.4), the volume fraction of the hard phase in the blend is between 0.33-0.55, which produces a lamellar structure in linear ABA triblock copolymers with symmetric end blocks. 70 The structure of the samples was studied using SAXS and these data are shown in Figures S8 and S9. The samples marked as 'LAM' in Figure 1 showed higher-order peaks consistent with a lamellar structure. The 'LAM' symmetry was also conrmed by TEM imaging for a blend with 10 vol% of PrC additive (= 0:28), corresponding to F_H=0.33, as shown in Figure S6. The samples marked as 'DIS' showed a primary peak and broad bump in intensity at higher q values, indicative of a poorly ordered structure without a clear symmetry. The grey shaded region in the SEBS/PS phase diagram marks conditions that produce macrophase separation, which were identied from the cloudy appearance of the Im as shown in Figure 1b. The macrophase-separated samples have SEBS-rich and PS-rich domains, where the SEBS-rich regions exhibit either the LAM or DIS structure.

As we can see from Figure 1a, the SEBS/PS blend undergoes phase separation at high values of and, as expected based on previous studies, ^{32,33} whereas the SEBS/PrC blend remained miscible for all and that were studied. The miscibility of the PrC additive with SEBS is also evident in tensile tests, as discussed in the next section. The Flory interaction parameter between PrC and PS is approximately -0.02 at 140 °C, based on the cloud point analysis of PrC/PS blends reported in previous works. ^{71,72} While this is only weakly negative, ⁶¹ it is evidently sucient to overcome entropic eects that drive phase separation of polymer additive from the conned lamellar morphology. SEBS/PrC blends also showed a lamellar morphology for almost all blends, except for the lowest values of

(0.18, 0.28) at = 0.4 where the disordered morphology was observed. This observation is at odds with a prior study of AB/C blends, where block B and homopolymer C were miscible due to hydrogen bonding interactions. AB In that study, the authors found that short-chain additives induce an order-order transition at lower loadings when compared to long-chain additives, an eect that was attributed to a more uniform distribution of the short-chain additive within the B domain. In the SEBS/PrC system, the short-chain PrC additives drive substantial swelling of the polystyrene domain at high loadings, as the appearance of the disordered morphology coincides with a large increase in domain periodicity. If the short-chain PrC additives are uniformly distributed within the domain, then the polystyrene chains in SEBS are highly stretched. This eect may introduce branching defects that disrupt the long-range order of domains.

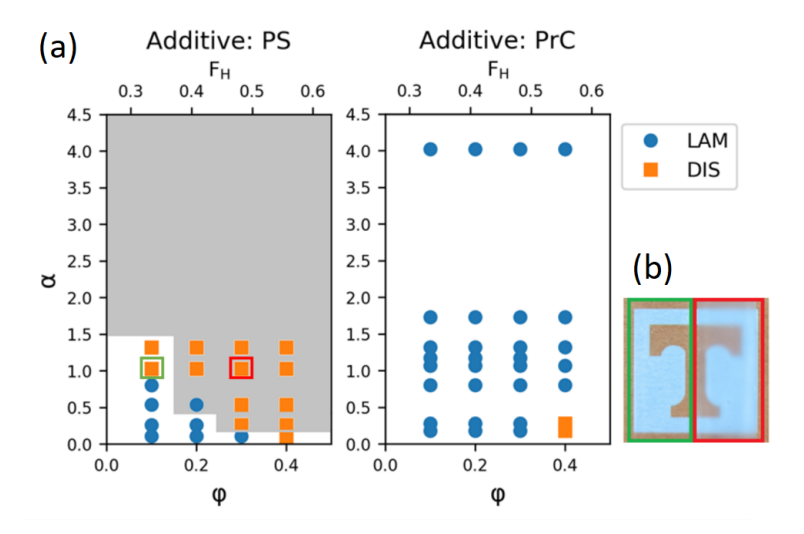


Figure 1: (a) Phase diagrams of SEBS/PS and SEBS/PrC blends as a function of relative chain length () and additive volume fraction (). (b) Films of miscible (green) and macrophase separated (red) blends, corresponding to the green and red squares in the SEBS/PS phase diagram, respectively. Shaded region indicates compositions that undergo macrophase separation.

Next, we examine how inuences the distribution of additive within the polystyrene domain of SEBS by plotting the lamellar periodicity L versus, as shown in Figure 2. This analysis is only applied to miscible blends. The value of L is calculated from the rst-order peak position, $L = 2/q^2$, where q^2 is the position of the primary SAXS peak. This calculation

of L is also applied for the disordered structures, where L reects an approximate correlation length rather than the lamellar periodicity. The size of the markers in Figure 2 corresponds to the uncertainty in periodicity, as explained in the Experimental section. Changes in additive distribution as a function of are inferred from changes in the dependence of L on .^{30,39,73} When the additive is distributed throughout the polystyrene domain, the polystyrene endblocks stretch and the domain width increases. This process either increases or decreases the width of the rubber domain, depending on how it impacts the interfacial area between junction points. When the additives are localized near the center of the polystyrene domain, the bilayer of polystyrene end-blocks is forced to expand and the domain width increases. This process does not impact the width of the rubber domain, so a greater increase in L is expected as increases, as opposed to the situation where the additive is uniformly distributed.

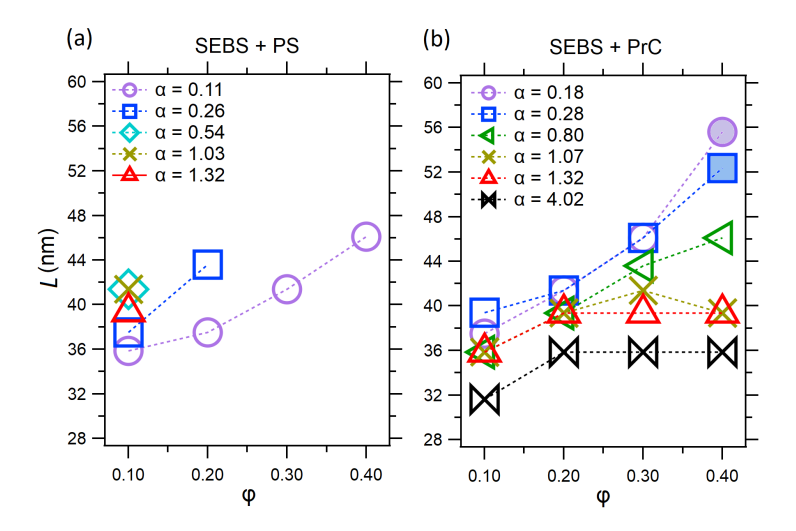


Figure 2: Periodicity (L) of miscible (a) SEBS/PS and (b) SEBS/PrC blends versus volume fraction of the additive () in the blend. Unlled markers represent blends with LAM structure, where L designates the lamellar periodicity. Filled markers represent blends with DIS structure, where L is an approximate correlation length.

For the SEBS/PS blends shown in Figure 2a, we observe a more pronounced increase in L with as increases, which is seen most clearly by comparing the trends for =0.11 and =0.26. This increase is indicative of the additive moving towards the center of the PS domains, that is, moving from the wet brush regime towards the dry brush regime,

with an increase in .^{30,36,74} No trend is identied with higher blends because the system phase separates when >0.1. In contrast, the SEBS/PrC blends shown in Figure 2b exhibit similar trends for L as a function of when is low (0.18 and 0.28), indicating that the additive distribution in this regime is not inuenced by . However, and as seen in Figure 2b, for = 0.80, 1.07, 1.32 and 4.02, L was reduced relative to the blends with = 0.18 and 0.28. Furthermore, when exceeded 0.8, L was invariant with for 0:2. While this behavior might suggest that the additive was phase separating from the SEBS, the blends remained optically clear. Alternatively, this behavior can be explained by an axial swelling (along the length of the lamellar domains) that is not directly captured by SAXS measurements. ^{30,36,39,74,75}

The trends for L with in both SEBS/PS and SEBS/PrC are distinct from some of the prior studies of lamellar AB/A and AB/C blends. In many AB/A blends with low, L may decline or stay approximately constant with increasing, reecting a uniform distribution of additive within the domain. 30,36,39,74 In one AB/A blend with low, L increased with as observed with SEBS/PS. However, in that example, the polymer type 'A' had functional groups that underwent weak hydrogen bonding, and the polymers 'A' and 'B' were strongly incompatible. 75 In AB/C blends with low, where blocks 'A' and 'C' can undergo hydrogen bonding, the trends for L with are conicting. One study reported that L increases with , similar to the trend observed in SEBS/PrC when < 1.39 Another study reported a decline in L with increasing .75 These studies diered in the degree of incompatibility between 'A' and 'B' blocks, where the latter system was more strongly incompatible. To our knowledge, there are no studies of BCP/polymer blends with attractive interactions that focus on > 1, the regime where we observe a constant L with increasing . Based on the results from prior literature, we conclude that the PrC additive is increasingly localized at the block copolymer interface as increases, but the underlying physics responsible for this trend are unclear. 30,36,39,74,75

Mechanical properties of SEBS/additive blends

Figure 3a-d shows the representative tensile plots for select SEBS/PS and SEBS/PrC blends with varying for = 0.1 and 0.3. The tensile behavior for SEBS with no additive is shown for comparison. The stress-strain curves for SEBS and miscible SEBS/additive blends show similar behaviour with three distinct regions: There is an initial region of elastic deformation, followed by yielding and a region of plastic deformation, and then a region showing strain hardening behavior before the sample breaks. Macroscopically, sample yielding is accompanied by formation of a distinct localized necked region which progresses through the sample with increasing strain. The necking is caused by fragmentation of the glassy domains, which allow the rubbery domains to deform elastically to a higher strain. 76 Once the sample is completely necked, a further increase in strain results in strain hardening behaviour, which is associated with additional breaking of the glassy fragments. The macrophase-separated SEBS/PS blend with =1.03 and =0.3, however, does not exhibit a distinct region between yielding and strain hardening (Figure 3b). This sample displayed uniform necking throughout the Im after yielding. The localized neck formation has been observed in BCP elastomers with globally-oriented lamellae and cylinders when the deforming force is applied parallel to the domain orientation. In morphologies where there are no continuous glassy domains to break, such as spherical morphologies where the minority component is glassy, yielding and localized necking are not observed during deformation. 77 The macrophaseseparated SEBS/PS blend is expected to have poor continuity in the glassy domains due to the disordered mesoscale structure, as shown in SAXS measurements (Figure S8), which explains the absence of localized necking.

Figures 4a-d reports the tensile properties of SEBS/PS and SEBS/PrC blends with = 0.1. For SEBS/PS blends, the blends with = 0.11, 0.54 and 0.81 show a higher modulus and yield stress than neat SEBS (Figures 4a-b). This is expected due to the increased content of glassy polymer. However, for the blends with = 1.03 and 1.32, the modulus and yield stress both drop to values approaching that of neat SEBS. This change in tensile

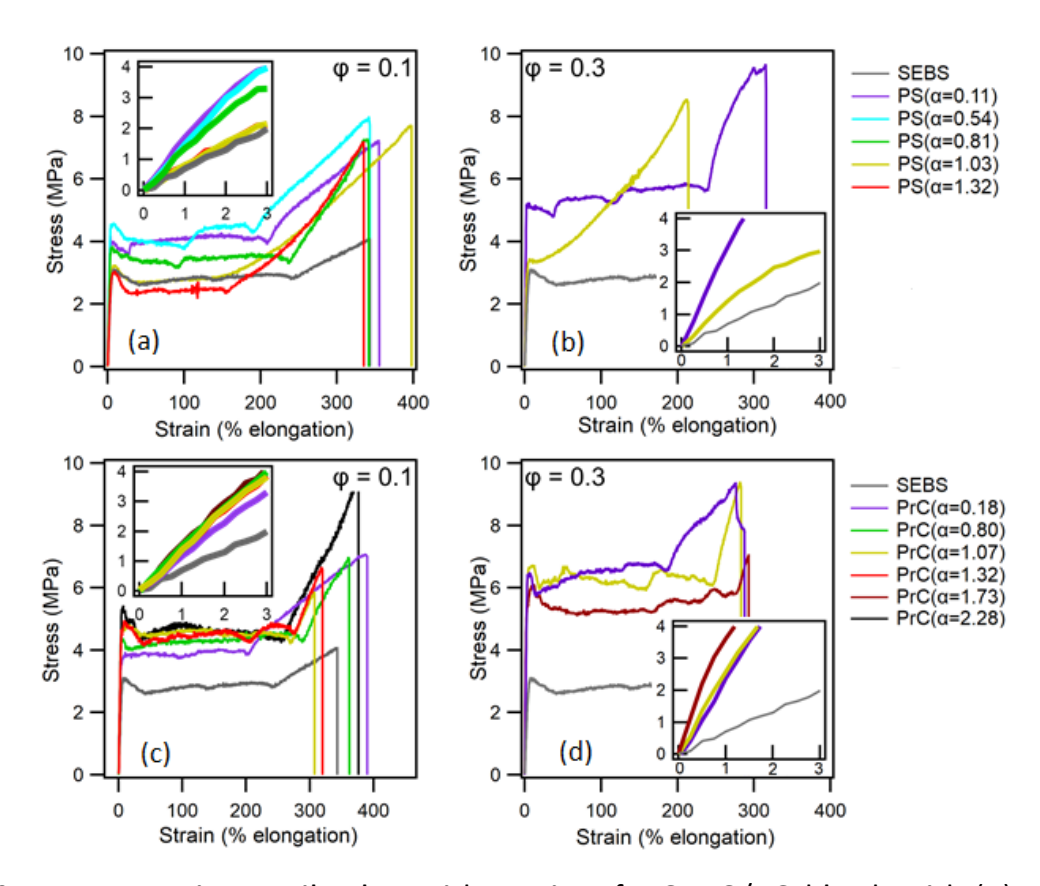


Figure 3: Representative tensile plots with varying for SEBS/PS blends with (a) =0.1 and (b) =0.3, and for SEBS/PrC blends with (c) =0.1 and (d) =0.3. The inset shows the stress-strain curves for values of strain up to 3%.

properties for blends with the same can be attributed to dierences in the mesoscale morphology: The blends with = 0.11, 0.54 and 0.81 have an ordered LAM structure, whereas the blends with = 1.03 and 1.32 have a disordered structure (Figure 1a and Figure S8). Previous works have also reported that microphase-separated BCPs with long-range order show better mechanical performance compared to those with poorly-ordered structures. 78,79 At low, the modulus and yield stress of SEBS/PrC blends are similar to those of SEBS/PS blends. However, the properties of the SEBS/PrC blends do not decline with increasing, which can be attributed to the well-dened LAM structure (Figure 1a). The toughnesses of neat SEBS and all of the miscible SEBS/additive blends are similar within the uncertainty of the measurements.

Figures 3b and 3d shows representative tensile plots for SEBS/PS and SEBS/PrC blends

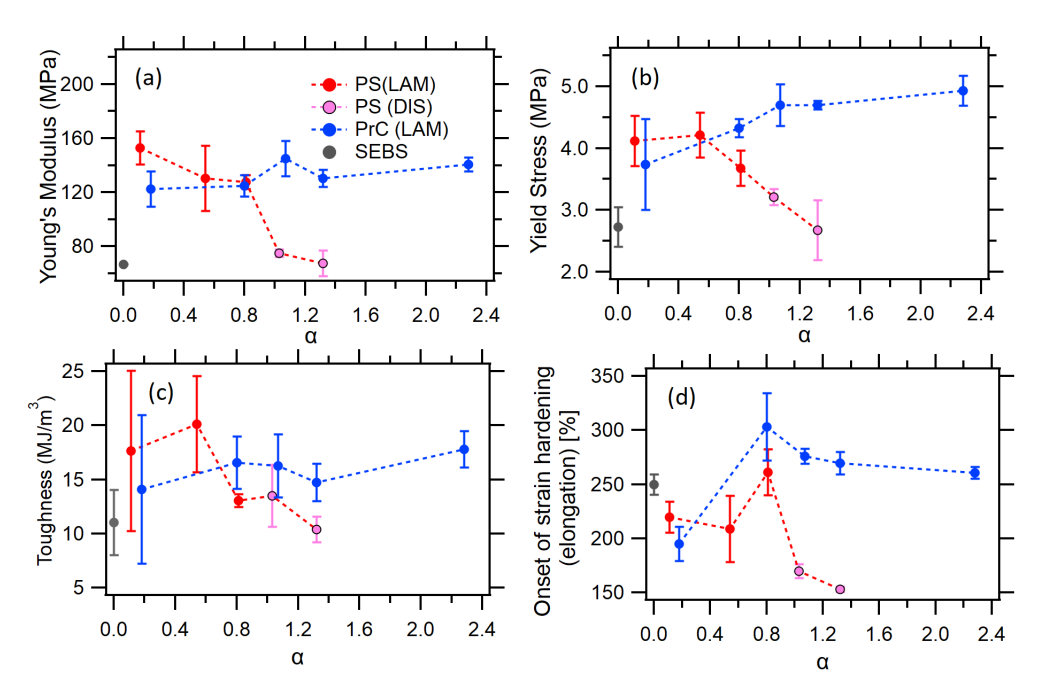


Figure 4: Mechanical properties as a function of for SEBS/PS and SEBS/PrC blends, = 0:1. The error bars denote 1 standard deviation based on four measurements. The properties of neat SEBS are marked by the grey circle (plotted at = 0).

with =0.3, and Figure S11 summarizes the tensile properties. The SEBS/PS blend with =0.11 is miscible and assembles into the LAM structure at = 0:3, and compared with = 0:1, the yield stress and modulus are increased with little impact on toughness. A similar trend is observed as is increased from 0.1 to 0.3 for SEBS/PrC blends with = 0.18, 1.07 and 1.73, all of which assembled into the LAM structure, despite signicant dierences in how L changes with (Figure 2b). The SEBS/PS blends with =1.03 are macrophase-separated at = 0:3, and consequently, the modulus, yield stress and toughness are all reduced relative to SEBS/PS blends with = 0:11.

Prior studies of BCP mechanics have shown that modulus, yield stress, and toughness all depend on the interfacial curvature of the domains. ^{20,80,81} BCPs with continuity in the rubbery domain, which happens when the minority glassy domain has convex curvature, oer ductility while discontinuity in the rubbery domains produces a brittle material. Adhikari et al. and Huy et al. compared mechanical properties of polystyrene-b-poly(butadiene)-b-polystyrene (SBS) with the same volume fraction of styrene but dierent morphologies. ^{80,81}

These works showed that SBS with discontinuous rubbery domains had a higher modulus and yield stress, but a drastic decline in toughness compared to SBS with lamellar morphology. Whether blending changes the interfacial curvature of SEBS depends on how the additive swells the domain, which is determined by how it is distributed within the domain. ⁴⁸ The fact that SEBS/PrC blends have similar tensile behavior for a broad range of (at constant) indicates that these additives do not change interfacial curvature in a way that disrupts continuity of rubber domain as is increased from 0.1 (F_H =0.33) to 0.3 (F_H =0.48). Thus, when blending SEBS with PrC additives, it is possible to create a miscible blend with ordered lamellar structures and good continuity in the rubbery domain for a broad range of and additive loading up to = 0:3. This provides the opportunity to prepare blend systems that have a high modulus and high yield stress without loss of toughness.

Figure 4d shows the dependence of the onset of strain hardening, which happens after the sample is completely necked, with . SEBS/PS blends with = 1.03 and 1.32, which have a disordered structure (Figure 1a), show an onset of strain hardening at a lower strain compared to the blends with LAM structures. Between yielding and the onset of strain hardening, deformation occurs through propagation of the necked region by fragmenting the PS domains. ⁷⁶ Thus, it makes sense that blends with poorly-ordered structures would be completely necked at lower strains, as it is easier to break apart an already fragmented glassy domain. The onset of strain hardening was also sensitive to the molecular weight of the additive, where blends with low (< 0:8) showed the onset at lower strains than those with higher . This observation suggests that low molecular weight additives make it easier to break apart the glassy domains under stress, perhaps due to a plasticizing eect.

From Figures 1, 3 and 4, we see that for higher values of , the phase behavior and mechanical properties of SEBS/PS and SEBS/PrC blends are quite dierent. However, when the SEBS/polymer blends are miscible and the morphology is LAM, the same modulus, yield stress and toughness are achieved irrespective of the type of additive. In consideration of tensile properties at ambient temperature, there does not seem to be an advantage of PrC

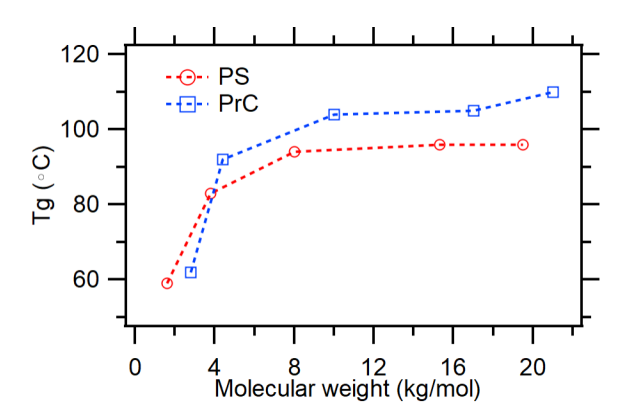


Figure 5: T_g of PS and PrC additives as a function of molecular weight, from DSC measurements.

over PS additives at low loadings (= 0:1), however, this may change at elevated temperatures: T_g is generally depressed as molecular weight is reduced, and miscible SEBS/PS blends with an ordered LAM structure are only achieved when the PS additive has a low molecular weight. Figure 5 reports the T_g , which was determined by DSC, of PS and PrC additives as a function of molecular weight. The T_g of PrC is higher relative to that of PS by approximately 10 K for all molecular weights in excess of 8 kg/mol. Both polymers show a drop in T_g when the molecular weight falls below approximately 8 kg/mol. Consequently, blends with low values are expected to depress the T_g of the glassy domain.

The T_g of the glassy domain in select SEBS/additive blends, using and values where both PS and PrC are miscible, was determined by DMA and is summarized in Table 2. Note that DSC could not detect T_g of the glassy domain in neat SEBS or SEBS/additive blends, as the T_g of the polystyrene block is signicantly broadened by mixing with the rubbery midblock. Relative to neat SEBS, the T_g of the glassy domain was depressed in SEBS/PS blends with = 0:1 and = 0:11, but slightly elevated as was increased to 0.54 and 1.03. However, the T_g of the glassy domain was slightly elevated in SEBS/PrC blends with = 0:1 and = 0:18, and it increased further as was increased to 0.63 and 1.07. The slight elevation for = 0:18 is surprising, as the T_g of this additive (ca. 60 °C) was signicantly depressed relative to that of the polystyrene block in SEBS (ca. 100 °C). However, in addition to molecular weight eects, the T_g of the glassy domain is also inuenced

by the strength of energetic interactions between the additive and the polystyrene block in SEBS. The attractive interaction between PrC and the polystyrene block could elevate the Tg of the glassy domain. $^{84}\ \text{To}\,$ interrogate this point, we compared the predicted T_g of the glassy domain using the Fox equation (Equation 2), which is applicable for polymer blends with weak intermolecular interactions, with the measured value for each SEBS/additive blend. The outcomes are shown in Table 2. The $T_{g,PS\ block}$ used for the calculation is the T_g of the polystyrene block measured from neat SEBS using DMA, which was found to be 102 °C. The T_{g,additive} was measured with DSC. The weight fraction of additive (w_{additive}) is based on the proportions of polystyrene and additive in the glassy domain, which is 0.3 and 0.325 for PS and PrC additives, respectively, for =0.1. We note that apart from the eect of any energetic interactions, the experimental and predicted values are expected to be dierent as the Fox equation does not account for connement in a self-assembled domain and the glass transitions of additive and polystyrene block are measured with dierent techniques. With these qualiers in mind, the discrepancy between experimental and predicted $\rm T_{\rm g}$ is 4-6 K $\,$ for SEBS/PS blends and 9-12 K for SEBS/PrC blends, indicating that attractive interactions in the latter system may enhance the thermal stability.

$$\frac{1}{T_{g}(K)} = \frac{W_{additive}}{T_{g,additive}(K)} + \frac{1-W_{additive}}{T_{g,PS block}(K)}$$
(2)

We further examined the thermal stability of SEBS/additive blends by performing tensile tests at an elevated temperature. Figure 6 shows stress-strain curves for blends with =0.1 at 80° C. The modulus obtained from the linear elastic region is listed in Table 2. For the SEBS/PS blends, the modulus when =0.11 is similar to that of neat SEBS (5 MPa), despite having a higher volume fraction of polystyrene. This softening is a consequence of the depressed T_g of the glassy domain, as seen in Table 2. As increases to 0.54 and 1.03, the modulus increases to 50 and 23 MPa, respectively. In these blends, the T_g of the glassy domain is similar to that of neat SEBS, so the improvement in modulus partly reects the higher content of glassy material. As observed with room temperature tensile

Table 2: Experimental and predicted values of T_g for the glassy domain of SEBS/additive blends at =0.1, and experimental modulus of SEBS and SEBS/additive blends with =0.1 at 80° C.

Additive type		Experimental T _g (°C)	Predicted T _g (°C)	Modulus at 80 °C (MPa)
-	-	102	102	8
PS	0.11	92	88	5
PS	0.54	106	99	50
PS	1.03	106	100	23
PrC	0.18	105	92	60
PrC	0.63	112	102	66
PrC	1.07	111	103	52

Experimental T_g is from the tan peak in DMA. Predicted T_g is from the Fox equation, using the additive T_g from DSC and the polystyrene block T_g from DMA of neat SEBS.

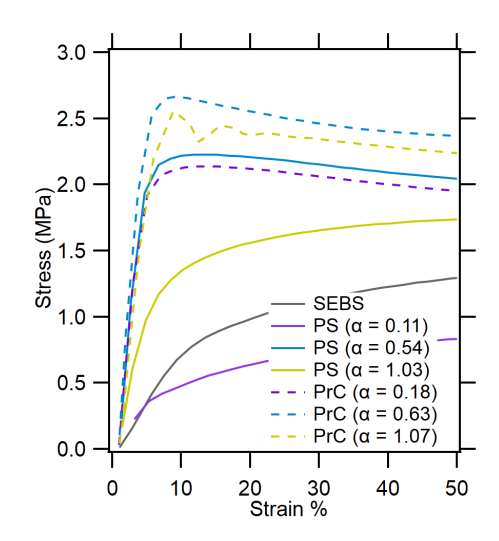


Figure 6: Stress-strain curves for SEBS and SEBS/additive blends (=0.1) at 80 °C.

tests, SEBS/PS blends with LAM order (= 0:54) have a higher modulus than those with a disordered structure (= 1:03). This can be explained by dierences in the degree of structural order, where the LAM structure produces a higher modulus than the disordered structure. For the SEBS/PrC blends, the modulus is in the vicinity of 60 MPa for all . These results show that miscible polymer additives that elevate the T_g of the glassy domain and produce a well-ordered mesocale structure can improve the thermal stability of SEBS.

Conclusions

We tuned the enthalpic and entropic interactions between SEBS and polymeric additives to understand the impacts on phase behavior, morphology, tensile properties, and thermal stability. In the case of SEBS/PS blends, where PS is an athermal additive for the polystyrene block in SEBS, the constituents were only miscible for low and . Consequently, there was an extremely narrow range of conditions that produced a single-phase blend with both a well-ordered morphology and a glassy T_g near 100 °C, leading to good mechanical properties at low and moderate temperatures. In SEBS/PrC blends, where PrC is a thermal additive for the polystyrene block in SEBS (Prc/PS = 0:02 at 140 °C), the constituents were miscible for the entire range of (0-0.4) and (0.1-4) that were studied. Nearly all SEBS/PrC blends assembled into well-ordered lamellar structures with continuity in the rubber phase, so the mechanical properties were largely controlled by (independent of), and the glassy PrC additive increased modulus and yield strength without compromising toughness. Furthermore, the PrC additive enhanced the thermal stability of the glassy domain, leading to good mechanical properties at elevated temperature. These results show that the PrCs are suitable additives to tailor the mechanical properties and expand the service window of styrenic BCP thermoplastics.

Acknowledgement

The authors thank the National Science Foundation for nancial support under Award No. DMR-1905487. SAXS measurements were enabled by the Major Research Instrumentation program of the National Science Foundation under Award No. DMR-1827474. Mechanical and thermal characterizations were performed at the University of Tennessee Polymer Characterization Laboratory.

Supporting Information Available

for PS/PrC; GPC and NMR for SEBS; GPC and NMR for each PrC, along with summary of key characteristics; SAXS and TEM of SEBS; TEM of a SEBS/PrC blend; SAXS measurements for as-cast versus annealed SEBS/PS blends; SAXS of all SEBS/PS and SEBS/PrC blends; Domain periodicity of SEBS/PS and SEBS/PrC blends; Tensile properties of select blends with = 0:3.

References

- (1) Puskas, J. E.; Antony, P.; El Fray, M.; Altstädt, V. The eect of hard and soft segment composition and molecular architecture on the morphology and mechanical properties of polystyrene-polyisobutylene thermoplastic elastomeric block copolymers. European Polymer Journal 2003, 39, 20412049, DOI: 10.1016/S0014-3057(03)00130-7.
- (2) Mori, Y.; Lim, L. S.; Bates, F. S. Consequences of molecular bridging in lamellaeforming triblock/pentablock copolymer blends. Macromolecules 2003, 36, 98799888, DOI: 10.1021/ma035300g.
- (3) Bates, C. M.; Bates, F. S. 50th anniversary perspective: Block polymers-pure potential. Macromolecules 2017, 50, 322, DOI: 10.1021/acs.macromol.6b02355.
- (4) Wang, W.; Lu, W.; Goodwin, A.; Wang, H.; Yin, P.; Kang, N. G.; Hong, K.; Mays, J. W. Recent advances in thermoplastic elastomers from living polymerizations: Macromolecular architectures and supramolecular chemistry. Progress in Polymer Science 2019, 95, 131, DOI: 10.1016/j.progpolymsci.2019.04.002.
- (5) Rahman, M. A.; Bowland, C.; Ge, S.; Acharya, S. R.; Kim, S.; Cooper, V. R.; Chelsea Chen, X.; Irle, S.; Sokolov, A. P.; Savara, A.; Saito, T. Design of tough adhesive from commodity thermoplastics through dynamic crosslinking. Science Advances 2021, 7, 112, DOI: 10.1126/sciadv.abk2451.

- (6) Beecher, J. F.; Marker, L.; Bradford, R. D.; Aggarwal, S. L. Morphology and mechanical behavior of block polymers. Journal of Polymer Science Part C: Polymer Symposia 1969, 26, 117134, DOI: 10.1002/polc.5070260108.
- (7) Hsiue, G. H.; Chen, D. J.; Liew, Y. K. Stress relaxation and the domain structure of thermoplastic elastomer. Journal of Applied Polymer Science 1988, 35, 9951002, DOI: 10.1002/app.1988.070350414.
- (8) Yamaoka, I.; Kimura, M. Eects of morphology on mechanical properties of a SBS triblock copolymer. Polymer 1993, 34, 43994409, DOI: 10.1016/0032-3861(93)90146-2.
- (9) McKay, K. W.; Gros, W. A.; Diehl, C. F. The inuence of styreneâ€"butadiene diblock copolymer on styreneâ€"butadieneâ€"styrene triblock copolymer viscoelastic properties and product performance. Journal of Applied Polymer Science 1995, 56, 947958, DOI: 10.1002/app.1995.070560808.
- (10) Ghosh, S.; Khastgir, D.; Bhowmick, A. K. Phase modication of SEBS block copolymer by dierent additives and its eect on morphology, mechanical and dynamic mechanical properties. Journal of Applied Polymer Science 1998, 67, 20152025, DOI: 10.1002/(SICI)1097-4628(19980321)67:12<2015::AID-APP7>3.0.CO;2-P.
- (11) Hotta, A.; Clarke, S. M.; Terentjev, E. M. Stress relaxation in transient networks of symmetric triblock styrene-isoprene-styrene copolymer. Macromolecules 2002, 35, 271 277, DOI: 10.1021/ma001976z.
- (12) Lietz, S.; Yang, J. L.; Bosch, E.; Sandler, J. K.; Zhang, Z.; Altstädt, V. Improvement of the mechanical properties and creep resistance of SBS block copolymers by nanoclay Ilers. Macromolecular Materials and Engineering 2007, 292, 2332, DOI: 10.1002/mame.200600280.

- (13) Xu, J.; Zhang, A.; Zhou, T.; Cao, X.; Xie, Z. A study on thermal oxidation mechanism of styrene-butadiene-styrene block copolymer (SBS). Polymer Degradation and Stability 2007, 92, 16821691, DOI: 10.1016/j.polymdegradstab.2007.06.008.
- (14) JuÆrez, D.; Ferrand, S.; Fenollar, O.; Fombuena, V.; Balart, R. Improvement of thermal inertia of styrene-ethylene/butylene-styrene (SEBS) polymers by addition of microencapsulated phase change materials (PCMs). European Polymer Journal 2011, 47, 153161, DOI: 10.1016/j.eurpolymj.2010.11.004.
- (15) Pantoja, M.; Jian, P. Z.; Cakmak, M.; Cavicchi, K. A. Shape Memory Properties of Polystyrene- block-poly(ethylene- co-butylene)- block-polystyrene (SEBS) ABA Triblock Copolymer Thermoplastic Elastomers. ACS Applied Polymer Materials 2019, 1, 414424, DOI: 10.1021/acsapm.8b00139.
- (16) Bates, F. S.; Fredrickson, G. H.; Hucul, D.; Hahn, S. F. PCHE-based pentablock copolymers: Evolution of a new plastic. AIChE Journal 2001, 47, 762765, DOI: 10.1002/aic.690470402.
- (17) Karatasos, K.; Anastasiadis, S. H.; Pakula, T.; Watanabe, H. On the loops-to-bridges ratio in ordered triblock copolymers: An investigation by dielectric relaxation spectroscopy and computer simulations. Macromolecules 2000, 33, 523541, DOI: 10.1021/ma991397y.
- (18) Spontak, R. J.; Smith, S. D. Perfectly-alternating linear (AB)n multiblock copolymers:

 Eect of molecular design on morphology and properties. Journal of Polymer Science,

 Part B: Polymer Physics 2001, 39, 947955, DOI: 10.1002/polb.1070.
- (19) Smith, S. D.; Spontak, R. J.; Satkowski, M. M.; Ashraf, A.; Heape, A. K.; Lin, J. S. Microphase-separated poly(styrene-b-isoprene)n multiblock copolymers with constant block lengths. Polymer 1994, 35, 45274536, DOI: 10.1016/0032-3861(94)90798-6.

- (20) Shi, W.; Lynd, N. A.; Montarnal, D.; Luo, Y.; Fredrickson, G. H.; Kramer, E. J.; Ntaras, C.; Avgeropoulos, A.; Hexemer, A. Toward strong thermoplastic elastomers with asymmetric miktoarm block copolymer architectures. Macromolecules 2014, 47, 20372043, DOI: 10.1021/ma402566g.
- (21) Shi, W.; Hamilton, A. L.; Delaney, K. T.; Fredrickson, G. H.; Kramer, E. J.; Ntaras, C.; Avgeropoulos, A.; Lynd, N. A. Creating extremely asymmetric lamellar structures via uctuation-assisted unbinding of miktoarm star block copolymer alloys. Journal of the American Chemical Society 2015, 137, 61606163, DOI: 10.1021/jacs.5b02881.
- (22) Shi, W.; Hamilton, A. L.; Delaney, K. T.; Fredrickson, G. H.; Kramer, E. J.; Ntaras, C.; Avgeropoulos, A.; Lynd, N. A.; Demassieux, Q.; Creton, C. Aperiodic "Bricks and Mortar" Mesophase: a New Equilibrium State of Soft Matter and Application as a Sti Thermoplastic Elastomer. Macromolecules 2015, 48, 53785384, DOI: 10.1021/acs.macromol.5b01210.
- (23) Kawarazaki, I.; Hayashi, M. Enhancement of Mechanical Properties of ABA Triblock Copolymer-Based Elastomers by Incorporating Partial Cross-Links on the Soft Bridge Chains. ACS Applied Polymer Materials 2021, 3, 12711275, DOI: 10.1021/acsapm.1c00026.
- (24) Hayashi, M.; Matsushima, S.; Noro, A.; Matsushita, Y. Mechanical property enhancement of ABA block copolymer-based elastomers by incorporating transient cross-links into soft middle block. Macromolecules 2015, 48, 421431, DOI: 10.1021/ma502239w.
- (25) Liu, B.; Chen, X.; Spiering, G. A.; Moore, R. B.; Long, T. E. Quadruple Hydrogen Bond-Containing A-AB-A Triblock Copolymers: Probing the Inuence of Hydrogen Bonding in the Central Block. Molecules 2021, 26, 4705, DOI: 10.3390/molecules26154705.
- (26) Watts, A.; Hillmyer, M. A. Aliphatic Polyester Thermoplastic Elastomers Contain-

- ing Hydrogen-Bonding Ureidopyrimidinone Endgroups. Biomacromolecules 2019, 20, 25982609, DOI: 10.1021/acs.biomac.9b00411.
- (27) Jiang, F.; Fang, C.; Zhang, J.; Wang, W.; Wang, Z. Triblock Copolymer Elastomers with Enhanced Mechanical Properties Synthesized by RAFT Polymerization and Subsequent Quaternization through Incorporation of a Comonomer with Imidazole Groups of about 2.0 Mass Percentage. Macromolecules 2017, 50, 62186226, DOI: 10.1021/acs.macromol.7b01414.
- (28) Kajita, T.; Tanaka, H.; Noro, A.; Matsushita, Y.; Nozawa, A.; Isobe, K.; Oda, R.; Hashimoto, S. Extremely tough block polymer-based thermoplastic elastomers with strongly associated but dynamically responsive noncovalent cross-links. Polymer 2021, 217, 16, DOI: 10.1016/j.polymer.2021.123419.
- (29) Choi, C.; Ahn, S.; Kim, J. K. Diverse Morphologies of Block Copolymers by Blending with Homo (and Co) Polymers. Macromolecules 2020, 53, 45774580, DOI: 10.1021/acs.macromol.0c00545.
- (30) Winey, K. I.; Thomas, E. L.; Fetters, L. J. Swelling a Lamellar Diblock Copolymer with Homopolymer: Inuences of Homopolymer Concentration and Molecular Weight.

 Macromolecules 1991, 24, 61826188, DOI: 10.1021/ma00023a020.
- (31) Koizumi, S.; Hasegawa, H.; Hashimoto, T. Spatial Distribution of Homopolymers in Block Copolymer Microdomains As Observed by a Combined SANS and SAXS Method.

 Macromolecules 1994, 27, 78937906, DOI: 10.1021/ma00104a053.
- (32) Winey, K. I.; Thomas, E. L.; Fetters, L. J. Isothermal Morphology Diagrams for Binary Blends of Diblock Copolymer and Homopolymer. Macromolecules 1992, 25, 26452650, DOI: 10.1021/ma00036a014.
- (33) Matsen, M. W. New fast SCFT algorithm applied to binary diblock copolymer homopolymer blends. Macromolecules 2003, 36, 96479657, DOI: 10.1021/ma0349377.

- (34) Matsen, M. Phase Behaviour of Block Copolymer/Homopolymer Blends. Macromolecules 1995, 28, 57655773, DOI: 10.1021/ma00121a011.
- (35) Winey, K. I.; Thomas, E. L.; Fetters, L. J. Ordered morphologies in binary blends of diblock copolymer and homopolymer and characterization of their intermaterial dividing surfaces. The Journal of Chemical Physics 1991, 95, 93679375, DOI: 10.1063/1.461164.
- (36) Tanaka, H.; Hascgawa, H.; Hashimoto, T. Ordered Structure in Mixtures of a Block Copolymer and Homopolymers. 1. Solubilization of Low Molecular Weight Homopolymers. Macromolecules 1991, 24, 240251, DOI: 10.1021/ma00001a037.
- (37) Jeong, U.; Ryu, D. Y.; Kho, D. H.; Kim, J. K.; Goldbach, J. T.; Kim, D. H.; Russell, T. P. Enhancement in the Orientation of the Microdomain in Block Copolymer Thin Films upon the Addition of Homopolymer. Advanced Materials 2004, 16, 533536, DOI: 10.1002/adma.200306113.
- (38) Koizumi, S.; Hasegawa, H.; Hashimoto, T. Ordered Stuctures of Block Copolymer/Homopolymer Mixtures. 5. Interplay of Macro- and Microphase Transitions. 1994, 80, 65326540.
- (39) Sunday, D. F.; Hannon, A. F.; Tein, S.; Kline, R. J. Thermodynamic and Morphological Behavior of Block Copolymer Blends with Thermal Polymer Additives. Macromolecules 2016, 49, 48984908, DOI: 10.1021/acs.macromol.6b00651.
- (40) Lee, J. H.; Balsara, N. P.; Chakraborty, A. K.; Krishnamoorti, R.; Hammouda, B. Thermodynamics and phase behavior of block copolymer/homopolymer blends with attractive and repulsive interactions. Macromolecules 2002, 35, 77487757, DOI: 10.1021/ma020361u.
- (41) Tirumala, V. R.; Daga, V.; Bosse, A. W.; Romang, A.; Ilavsky, J.; Lin, E. K.; Watkins, J. J. Well-ordered polymer melts with 5 nm lamellar domains from blends

- of a disordered block copolymer and a selectively associating homopolymer of low or high molar mass. Macromolecules 2008, 41, 79787985, DOI: 10.1021/ma801124n.
- (42) Erukhimovich, I.; de la Cruz, M. O. Tuning Block Copolymer Phase Behavior with a Selectively Associating Homopolymer Additive. 2004, 20832090, DOI: 10.1002/polb.
- (43) Hashimoto, T.; Kimishima, K.; Hasegawa, H. Self-Assembly and Patterns in Binary Mixtures of SI Block Copolymer and PPO. Macromolecules 1991, 24, 57045712, DOI: 10.1021/ma00020a034.
- (44) Adedeji, A.; Jamieson, A. M.; Hudson, S. D. Microphase vs. macrophase formation in homopolymer/block copolymer blends with exothermic interaction. Polymer 1995, 36, 27532760, DOI: 10.1016/0032-3861(95)93653-4.
- (45) Adedeji, A.; Hudson, S. D.; Jamieson, A. M. Enthalpy-enhanced microphase separation in homopolymer/block copolymer blends. Polymer 1997, 38, 737741, DOI: 10.1016/S0032-3861(96)00696-9.
- (46) Jeong, U.; Ryu, D. Y.; Kho, D. H.; Lee, D. H.; Kim, J. K.; Russell, T. P. Phase behavior of mixtures of block copolymer and homopolymers in thin lms and bulk.

 Macromolecules 2003, 36, 36263634, DOI: 10.1021/ma034179k.
- (47) Dobrosielska, K.; Wakao, S.; Takano, A.; Matsushita, Y. Nanophase-separated structures of AB block copolymer/C homopolymer blends with complementary hydrogen-bonding interactions. Macromolecules 2008, 41, 76957698, DOI: 10.1021/ma801330p.
- (48) Dobrosielska, K.; Wakao, S.; Suzuki, J.; Noda, K.; Takano, A.; Matsushita, Y. Eect of homopolymer molecular weight on nanophase-separated structures of AB block copolymer/C homopolymer blends with hydrogen-bonding interactions. Macromolecules 2009, 42, 70987102, DOI: 10.1021/ma901212p.

- (49) Tucker, P. S.; Paul, D. R. Simple Model for Enthalpic Eects in Homopolymer/Block Copolymer Blends. Macromolecules 1988, 21, 28012807, DOI: 10.1021/ma00187a027.
- (50) Tucker, P. S.; Barlow, J. W.; Paul, D. R. Molecular Weight Eects on Phase Behavior of Blends of Poly(phenylene oxide) with Styrenic Triblock Copolymers. Macromolecules 1988, 21, 27942800, DOI: 10.1021/ma00187a026.
- (51) Benabdelghani, Z.; Belkhiri, R.; Djadoun, S. Blends of poly(2,6-dimethyl-I,4-phenylene oxide)/ poly(styrene-co-methacrylic acid)/ poly(ethyl methacrylate-co-4-vinylpyridine). Polymer Bulletin 1995, 35, 329336.
- (52) Goh, S. H.; Lee, S. Y. Miscibility of poly(2,6-dimethyl-1,4-phenylene oxide) with iodinated polystyrene. European Polymer Journal 1989, 25, 997999, DOI: 10.1016/0014-3057(89)90127-4.
- (53) Fried, J. R.; MacKnight, W. J.; Karasz, F. E. Modeling of tensile properties of polymer blends: PPO / poly (styrene- co p chlorostyrene). Journal of Applied Physics 1979, 50, 60526060.
- (54) Stoelting, J.; Karasz, F. E.; Macknight, W. J. Dynamic Mechanical Properties of Poly(2,6-Dimethyl-I,4- Phenylene Ether)-Polystyrene Blends. Polymer Engineering And Science 1970, 10, 133138.
- (55) Shultz, A. R.; Beach, B. M. Thermo-Optical, Dierential Calorimetric, and Dynamic Viscoelastic Transitions in Poly(2,6-dimethyl-1,4-phenylene oxide) (PPO Resin) Blends with Poly-p-chlorostyrene and with Styrene-p- Chlorostyrene Statistical Copolymers. Macromolecule 1974, 7, 902909.
- (56) Chang, L. L.; Woo, E. M. Miscibility, Morphology, and Thermal Characterization of an Acrylic/Styrenic Blend System. Poly(cyclohexyl methacrylate) and Poly(a-methyl styrene). Polymer Journal 2001, 33, 1317.

- (57) Tucker, P. S.; Barlow, J. W.; Paul, D. R. Phase Behavior for Blends of Styrene Containing Triblock Copolymers with Poly(2,6-dimethyl-1,4-phenylene oxide). Journal Of Applied Polymer Science 1987, 34, 18171833, DOI: 10.1002/app.1987.070340504.
- (58) Tucker, P. S.; Barlow, J. W.; Paul, D. R. Thermal, Mechanical, and Morphological Analyses of Poly(2,6-dimethyl-I,4-phenyleneoxide) / Styrene-Butadiene-Styrene Blends. Macromolecules 1988, 21, 16781685.
- (59) Yu, X.; Wang, X.; Zhang, A.; Zhou, T. Inuence of processing conditions on mechanical properties of blends of styrenic block copolymer and poly(phenylene oxide): Miscibility and microdomain size. Journal of Applied Polymer Science 2018, 135, 18, DOI: 10.1002/app.46123.
- (60) Hay, S. Polymerization oxidative coupling: Discovery and Α. by commercialization of PPO and Noryl resins. Journal of Polymer Science, Part A: Polymer Chemistry 1998, 36, 505517, DOI: 10.1002/(SICI)1099-0518(199803)36:4<505::AID-POLA1>3.0.CO;2-O.
- (61) Nishimoto, M.; Keskkula, H.; Paul, D. R. Blends of Poly(styrene-co-acrylonitrile) and Methyl Methacrylate Based Copolymers. Macromolecules 1990, 23, 36333639, DOI: 10.1021/ma00217a016.
- (62) Chong, Y. F.; Goh, S. H. Miscibility of poly(tetrahydropyranyl-2-methacrylate) and poly(cyclohexyl methacrylate) with styrenic polymers. European Polymer Journal 1991, 27, 501504, DOI: 10.1016/0014-3057(91)90174-M.
- (63) Friedrich, C.; Schwarzwälder, C.; Riemann, R. E. Rheological and thermodynamic study of the miscible blend polystyrene/poly(cyclohexyl methacrylate). Polymer 1996, 37, 24992507, DOI: 10.1016/0032-3861(96)85365-1.
- (64) Khandpur, A. K.; Förster, S.; Bates, F. S.; Hamley, I. W.; Ryan, A. J.; Bras, W.; Almdal, K.; Mortensen, K. Polyisoprene-Polystyrene Diblock Copolymer Phase Dia-

- gram near the Order-Disorder Transition. Macromolecules 1995, 28, 87968806, DOI: 10.1021/ma00130a012.
- (65) Aden, B.; Kite, C. M.; Hopkins, B. W.; Zetterberg, A.; Lokitz, B. S.; Ankner, J. F.; Kilbey, S. M. Assessing Chemical Transformation of Reactive, Interfacial Thin Films Made of End-Tethered Poly(2-vinyl-4,4-dimethyl azlactone) (PVDMA) Chains. Macromolecules 2017, 50, 618630, DOI: 10.1021/acs.macromol.6b01999.
- (66) Kim, I.; Shi, R.; Choe, Y.; Kim, E. J.; Kim, B. J.; Qian, H. J.; Li, S. Stabilization of complex morphologies in highly disperse AB diblock copolymers. Polymer 2020, 198, 122519, DOI: 10.1016/j.polymer.2020.122519.
- (67) Lai, C.; Loo, Y. L.; Register, R. A.; Adamson, D. H. Dynamics of a thermoreversible transition between cylindrical and hexagonally perforated lamellar mesophases. Macromolecules 2005, 38, 70987104, DOI: 10.1021/ma050953n.
- (68) Mineart, K. P.; Jiang, X.; Jinnai, H.; Takahara, A.; Spontak, R. J. Morphological Investigation of Midblock-Sulfonated Block Ionomers Prepared from Solvents Diering in Polarity. Macromolecular Rapid Communications 2015, 10.1002/marc.201400627, 36, 432438, DOI: eprint: https://onlinelibrary.wiley.com/doi/pdf/10.1002/marc.201400627.
- (69) Hansen Solubility Parameters | Hansen Solubility Parameters. https://hansen-solubility.com/, Date Accessed: 06.26.2023.
- (70) Matsen, M. W. Equilibrium behavior of symmetric ABA triblock copolymer melts.

 Journal of Chemical Physics 1999, 111, 71397146, DOI: 10.1063/1.1289889.
- (71) Pomposo, J. A.; Mi'Tgica, A.; Areizaga, J.; Cortdzar, M. Modeling of the phase behavior of binary and ternary blends involving copolymers of styrŁne, methyl methacrylate and cyclohexyl methacrylate. Acta Polymerica 1998, 49, 301311, DOI: 10.1002/(SICI)1521-4044(199806)49:6<301::AID-APOL301>3.0.CO;2-T.

- (72) Callaghan, T. A.; Paul, D. R. Interaction Energies for Blends of Poly (methyl methacrylate), Polystyrene, and Poly(a-methylstyrene) by the Critical Molecular Weight Method. Macromolecules 1993, 26, 24392450.
- (73) Samant, S.; Basutkar, M.; Singh, M.; Masud, A.; Grabowski, C. A.; Kisslinger, K.; Strzalka, J.; Yuan, G.; Satija, S.; Apata, I.; Raghavan, D.; Durstock, M.; Karim, A. Eect of Molecular Weight and Layer Thickness on the Dielectric Breakdown Strength of Neat and Homopolymer Swollen Lamellar Block Copolymer Films. ACS Applied Polymer Materials 2020, 2, 30723083, DOI: 10.1021/acsapm.0c00127, Publisher: American Chemical Society.
- (74) Lin, Y.-H.; Shiu, C.-C.; Chen, T.-L.; Chen, H.-L.; Tsai, J.-C. Solubilization Behavior of Homopolymer in Its Blend with the Block Copolymer Displaying the Feature of Lower Critical Ordering Transition. Polymers 2021, 13, 3415, DOI: 10.3390/polym13193415, Number: 19 Publisher: Multidisciplinary Digital Publishing Institute.
- (75) Chen, S.-C.; Kuo, S.-W.; Jeng, U.-S.; Su, C.-J.; Chang, F.-C. On Modulating the Phase Behavior of Block Copolymer/Homopolymer Blends via Hydrogen Bonding. Macromolecules 2010, 43, 10831092, DOI: 10.1021/ma901729t, Publisher: American Chemical Society.
- (76) Cohen, Y.; Albalak, R. J.; Dair, B. J.; Capel, M. S.; Thomas, E. L. Deformation of oriented lamellar block copolymer Ims. Macromolecules 2000, 33, 65026516, DOI: 10.1021/ma000513q.
- (77) Honeker, C. C.; Thomas, E. L. Impact of morphological orientation in determining mechanical properties in triblock copolymer systems. Chemistry of Materials 1996, 8, 17021714, DOI: 10.1021/cm960146q.
- (78) Orimo, Y.; Hotta, A. Stress-strain behavior, elastic recovery, fracture points, and time-

- temperature superposition of an oot-possessing triblock copolymer. Macromolecules 2011, 44, 53105317, DOI: 10.1021/ma200087r.
- (79) Su, B.; Zhao, Y. s.; Chen, F.; Fu, Q. Eect of microdomain structure on the mechanical behavior of binary blends. Chinese Journal of Polymer Science (English Edition) 2015, 33, 964975, DOI: 10.1007/s10118-015-1649-4.
- (80) Huy, T. A.; Hai, L. H.; Adhikari, R.; Weidisch, R.; Michler, G. H.; Knoll, K. Inuence of interfacial structure on morphology and deformation behavior of SBS block copolymers. Polymer 2003, 44, 12371245, DOI: 10.1016/S0032-3861(02)00630-4.
- (81) Adhikari, R.; Michler, G. H.; Huy, T. A.; Ivan'Kova, E.; Godehardt, R.; Lebek, W.; Knoll, K. Correlation between molecular architecture, morphology, and deformation behaviour of styrene/butadiene block copolymers. Macromolecular Chemistry and Physics 2003, 204, 488499, DOI: 10.1002/macp.200390022.
- (82) Masson, J.-F.; Bundalo-Perc, S.; Delgado, A. Glass transitions and mixed phases in block SBS. Journal of Polymer Science Part B: Polymer Physics 2005, 43, 276279, DOI: 10.1002/polb.20319.
- (83) Wu, J. Physical Properties of Blends of Triblock Copolymer (SEBS) with Low Molar Mass Liquid Crystals. M.Sc. thesis, University of Akron, 2015.
- (84) Lu, X.; Weiss, R. A. Relationship between the Glass Transition Temperature and the Interaction Parameter of Miscible Binary Polymer Blends. Macromolecules 1992, 25, 32423246, DOI: 10.1007/978-1-4419-6247-8_12027.

Graphical TOC Entry

